J. Fluid Mech. (1986), *vol.* 163, *pp.* 227–256
Printed in Great Britain

Structural characteristics of a developing turbulent planar jet

By F. O. THOMAS
School of Mechanical and Aerospace Engineering, Oklahoma State University, Stillwater, Oklahoma

AND V. W. GOLDSCHMIDT
School of Mechanical Engineering, Purdue University, West Lafayette, Indiana

(Received 28 February 1984 and in revised form 5 August 1985)

An experimental study of the developing structural characteristics of a two-dimensional jet in an extremely quiet environment was performed. The jet, at an exit Reynolds number of 6000 and with fluctuation intensity under 0.2% at the mouth, was operated within a large anechoic room. Measurements of energy spectra, fluctuation phase angles and two-dimensionality led to the inference of structural patterns in the flow. These patterns are initially characterized by relatively strong symmetric modes exhibiting limited two-dimensionality and oriented parallel to the mouth of the jet. Subsequent downstream evolution led to the formation of an antisymmetric pattern beyond the jet potential core and the associated development of extended structures possessing a definite large lateral inclination. The results of this work suggest a developing large-scale structural pattern more complicated than previously supposed.

1. Introduction

Though the origin of the concept of large-scale structures in turbulent shear flows dates to Townsend (1956) and Grant (1958), the emphasis on the study of such structures in free shear flows seemed to commence in a real sense after work by Brown & Roshko (1971, 1974), Winant & Browand (1974) and Browand & Weidman (1976) in the plane mixing layer. Since that time there has been a gradual shift in the approach taken to turbulence research. A growing body of experimental evidence has led to a general recognition of large-scale coherent structures in free turbulent shear flows that were formerly thought to be fully random in nature. This has resulted in a departure from the traditional description of turbulence in the Reynolds sense (e.g. Hussain & Reynolds 1970; Alper & Liu 1978). Recent studies have been more concerned with the deterministic aspects of flows, as discussed in review articles by Laufer (1975), Davies & Yule (1975), Roshko (1976) and Cantwell (1981). Such works suggest the necessity of incorporating the coherent-structure dynamics in order to obtain a realistic model of turbulent shear flows.

Probably the strongest indication of coherent structure in the two-dimensional turbulent jet is the occurrence of negative correlation between longitudinal-velocity-fluctuation signals obtained simultaneously from laterally separated hot-wire probes on opposite sides of the jet centreline. Such correlation functions also typically exhibit an oscillatory behaviour in time. This phenomenon is well documented (see Goldschmidt & Bradshaw 1973; Weir & Bradshaw 1975; Everitt & Robins 1978;

Cervantes & Goldschmidt 1981; Oler & Goldschmidt 1982; and Antonia *et al.* 1983) and has been termed 'flapping', based on early interpretations which likened the motion of the jet to a flapping flag. Cervantes & Goldschmidt (1981) performed an extensive set of two-point correlation measurements of the longitudinal velocity fluctuation of a planar jet and showed that the apparent flapping frequency of the jet scaled in accord with local mean-flow similarity requirements. They interpreted this as indicative of a structural origin of the 'flapping' motion.

More recently Oler & Goldschmidt (1982) have also interpreted the flapping phenomenon as indicative of the occurrence of large-scale flow structures in the similarity region of the planar jet. In particular, the coherent structure was envisioned as a Kármán-vortex-street arrangement of eddy structures aligned in the direction of mean-flow homogeneity and convecting downstream. A kinematic model based upon such a structure was found capable of generating realistic time-mean streamwise and lateral velocities and Reynolds-stress magnitudes. In an experimental study Mumford (1982) obtained iso-correlation contours from two-point velocity correlations and also used digital pattern-recognition techniques to infer the structure of large eddies in the similarity region of a planar jet. Evidence was found for the existence of roller-like structures. The rollers were noted to be aligned either in the direction of mean-flow homogeneity or in the direction of strain associated with the mean-velocity gradient. Antonia *et al.* (1983) indicate that the results of correlation measurements of instantaneous velocity and temperature fields confirm the nature of the organized motion proposed by Oler & Goldschmidt (1982). They note, however, that this structure may be only one type of basic structure that occurs in two-dimensional jets, and suggest that various combinations of the structures detected by Mumford (1982) may coexist in the jet as well.

The purpose of this work is to document the growth and development of structural patterns associated with the large-scale structure in the two-dimensional turbulent jet. Thus an attempt is made to help clarify the role of initial conditions and coherent-structure interactions on subsequent flow development. Experimental results by a number of researchers (e.g. Bradshaw 1966; Flora & Goldschmidt 1969; Kleis & Foss 1974; Hussain & Clark 1977; Hussain & Zeda 1978; Hussain & Husain 1979; and Oster *et al.* 1977) have indicated that 'memory' effects of the initial instability may be felt to surprising distances downstream in free shear flows. Hence emphasis in the work to be reported was placed upon studying the development of structural patterns which are seen as characteristics of large-scale flow development. Such patterns are based upon measurements of the spectral evolution, characteristic wavelength, phase and two-dimensionality of longitudinal velocity fluctuations. A second, related goal of the work was to obtain additional information regarding the large-scale structure as it exists in the similarity region of the two-dimensional turbulent jet.

2. Experimental facility

A schematic diagram of the test set-up is shown in figure 1. The important features of the facility are its practically complete isolation from laboratory noise, and the extreme precautions taken to reduce any blower or duct disturbances from propagating to the plenum of the jet. To accomplish the first objective the jet was placed in a large cubic anechoic chamber with dimensions of 3.7 m (12 ft). The second objective was met through the use of the large annular muffler shown in figure 1 along with stilling sections. Details of the set-up are contained in Thomas (1983).

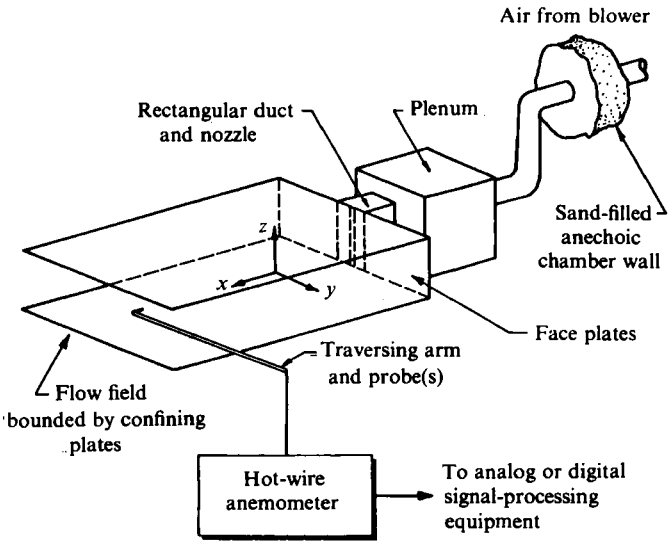

FIGURE 1. Schematic of the test set-up.

The Reynolds number of the exit flow from the $D = 0.64$ cm (0.25 in.) by $h = 30.48$ cm (12 in.) vertical slot was 6000, corresponding to an exit velocity of 15.24 m/s (50 ft/s). The initial velocity profiles were flat, exhibiting a 'top-hat' shape. The boundary layer at the nozzle exit agreed well with the Blasius flat-plate profile and exhibited a momentum thickness of 86 μm (0.0034 in.). Large sheet-steel horizontal flow-field confining plates (see figure 1) were used to maintain the two-dimensionality of the jet. Vertical face plates in the nozzle exit plane ensured that the entrained flow possessed a negligible axial velocity component. The conventional measure of widening and velocity decay in the region of mean-flow similarity yielded the following:

$$\frac{b}{D} = K_1\left(\frac{x}{D} - C_1\right) \tag{1}$$

and

$$\left(\frac{U_M}{U_0}\right)^{-2} = K_2\left(\frac{x}{D} - C_2\right), \tag{2}$$

where b = mean-velocity half-width, U_M = local centreline mean velocity, U_0 = exit mean velocity, K_1 = jet widening rate, $\mathrm{d}(b/D)/\mathrm{d}(x/D) = 0.10$, K_2 = jet mean-velocity decay rate, $\mathrm{d}(U_0^2/U_M^2)/\mathrm{d}(x/D) = 0.22$, C_1 = virtual origin based upon jet widening $= -3.2$, C_2 = virtual origin based upon mean-velocity decay $= -1.6$.

These mean-flow parameters were compared with others available in the literature and found to be generally typical of those reported, confirming that the jet was well behaved as far as mean-flow quantities are concerned.

The test facility was originally designed to evaluate the interaction of an acoustic disturbance with the jet. Preliminary results of that work were published in Thomas & Goldschmidt (1983). The results now presented are for the natural transition of the jet. It should be noted that it is generally recognized that jet flows are sensitive to external disturbances and are hence in some sense forced. These external disturbances such as noise, plenum resonance, thermal disturbances, can have an uncontrollable effect on initial conditions and modify the subsequent evolution

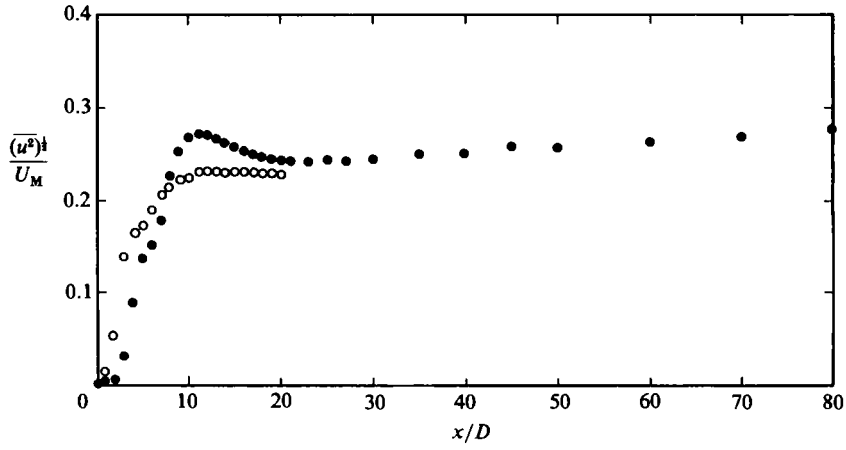

FIGURE 2. Longitudinal fluctuation intensity: ●, $y = 0$ (centreline); ○, $y = b(x/D)$ (shear layer).

of the coherent structure. The fact that the reported data were taken in an environment practically free from outside noise makes these results most unusual and revealing. To the authors' knowledge no study of the natural two-dimensional jet has gone to such extremes to minimize the occurrence of external disturbances. This should make the results more 'universal' in the sense that they are not dependent on individual laboratory peculiarities.

The instrumentation used consisted of conventional hot-wire-anemometry equipment and on-line digital data processing. Specifically TSI 1050 series anemometers were used in conjunction with DISA 55F11 conventional straight-wire probes which were operated in the constant-temperature mode. A Hewlett–Packard 5451-C Fast Fourier Analyzer System was used for all data acquisition and processing.

In the discussion that follows, representative data are first presented and then a descriptive model is proposed. The data are limited to spectral development of the longitudinal velocity fluctuations and to various correlations between longitudinal velocity fluctuations in different regions of the jet.

3. Characterizing data

3.1. *Jet spectral development*

The longitudinal velocity-fluctuation-intensity variation along the centreline of the jet and at $y/b = 1.0$ (i.e. 'shear layer') is shown in figure 2. As one may expect, the initial growth rate of fluctuations in the shear layer is more rapid than on the centreline and the fluctuations become fully developed sooner. The lateral distributions of longitudinal-fluctuation intensity at selected x/D stations are presented in figure 3. They demonstrate the growth of shear-layer fluctuations which evolve to exhibit profiles with well-documented shapes and levels already reported in the literature (see, for example, Bradbury 1965; Heskestad 1965; Robins 1973; Gutmark & Wygnanski 1976; Chambers 1977; Everitt & Robins 1978; Townsend 1956; and Thompson 1975).

Of more interest is the spectral development associated with the velocity fluctuations. It is well known that the laminar–turbulent transition of a free shear flow is initiated by the selective amplification of small disturbances (see, for example, Sato 1960; Sato & Kuriki 1961; Sato & Sakao 1964; Michalke 1965; Browand 1966;

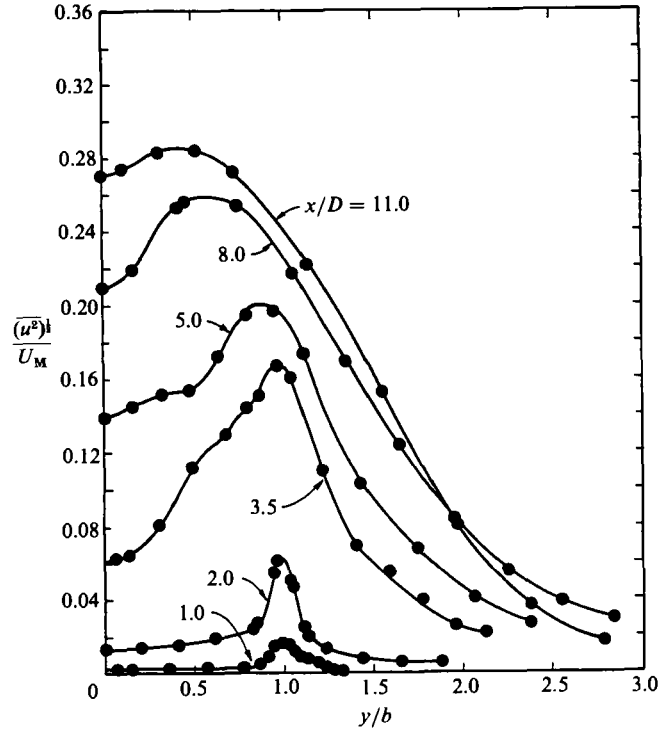

FIGURE 3. Lateral distribution of the longitudinal fluctuation intensity.

Freymuth 1966; and Mattingly & Criminale 1971). For a disturbance with an appropriate wavenumber, the disturbance grows exponentially in the flow direction.

Initial jet-shear-layer spectra are shown in figure 4 (*a*). The jet-shear-layer spectrum at $x/D = 1$ shows a number of very low-level peaks corresponding to disturbance modes present in the flow. Comparison of the spectra at $x/D = 1$ and 2 demonstrates the selective amplification of these spectral components based upon their frequency. Little interaction between modes is observed, as the amplitudes are small. Figure 5 shows that the velocity distribution across the shear layer at these x/D stations is closely approximated by a hyperbolic-tangent profile. Michalke (1965) investigated the stability characteristics of the hyperbolic-tangent velocity profile for spatially amplified disturbances. Theoretical spatial amplification rates from Michalke's (1965) theory and experimentally measured values obtained for the growth of different spectral modes are compared in figure 6: $\beta_r = 2\pi f\delta/U_0$ is a dimensionless frequency where the lengthscale δ is the shear-layer thickness, and $-\alpha_i$ is the spatial growth rate of disturbances. The agreement is good, though the measured amplification rates are somewhat lower than those predicted by theory.

The shear-layer spectrum at $x/D = 3$ differs markedly from that at 2. The shear-layer-velocity fluctuations have grown to amplitudes which are evidently sufficiently high to invalidate linear theory. In fact a criterion for the onset of nonlinear effects noted by Sato (1960) requiring that $(\overline{u^2}(f))^{\frac{1}{2}}/U_M > 4\,\%$ is satisfied and distortion of the mean-velocity profile occurs ($\overline{u^2}(f)$ corresponds to the mean square of the fluctuation component at frequency f). Before discussing in some detail the effect of nonlinear interaction of fluctuations on the spectrum, some consideration will be given to related work involving free-shear-flow transition.

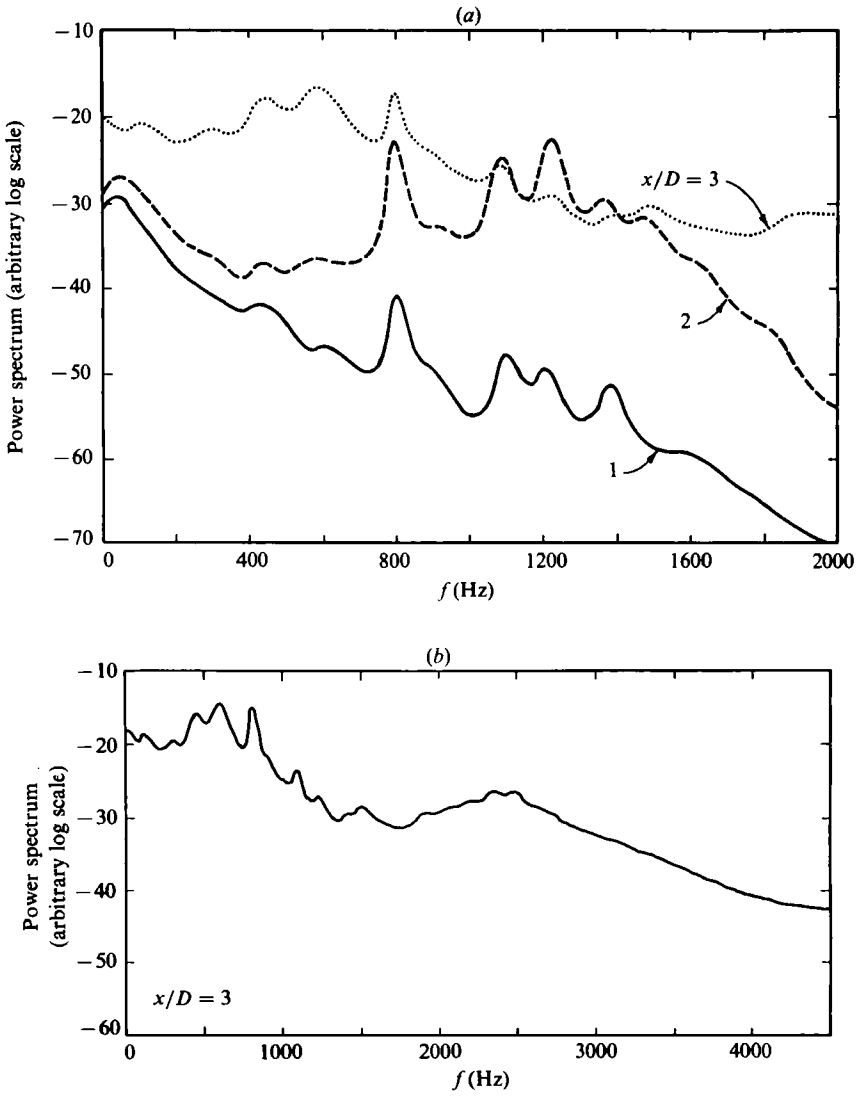

FIGURE 4. (*a*) Initial shear-layer spectra. (*b*) Shear-layer spectrum at $x/D = 3$.

Miksad (1972, 1973) performed experiments on the nonlinear aspects of free-shear-layer transition. Two streams of air at different velocities merged beyond a splitter plate to form a two-dimensional mixing layer. Many features present in the jet-shear-layer spectra to be presented closely parallel those described by Miksad.

Miksad's results show that the nonlinear interactions between two disturbances at frequencies f_1 and f_2 result in the creation of sum and difference spectral modes $(f_2 \pm f_1)$. Harmonics and subharmonics of f_1 and f_2 are also generated. All modes were noted by Miksad (1972, 1973) to interact to form fluctuations at frequencies $(nf_2/m) \pm (pf_1/q)$; $n, p = 1, 2, 3, \ldots, m, q = 1, 2$. The interaction between modes was found to be most effective when the frequencies and amplitudes of the interacting components were similar. In addition, the growth of a particular spectral component was noted to be suppressed by the presence of another strong component.

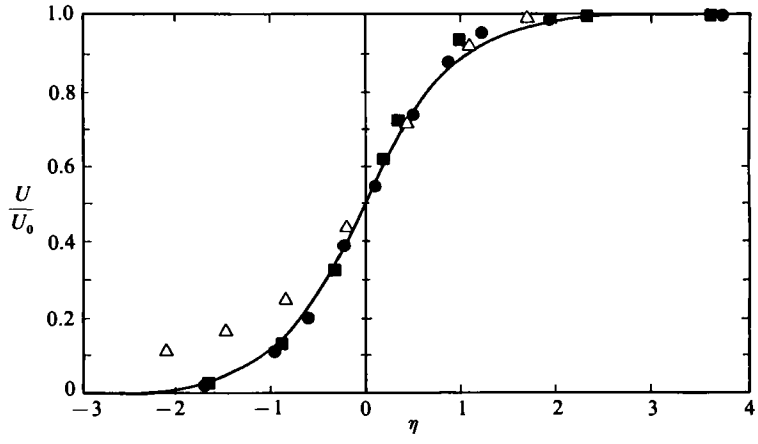

FIGURE 5. Initial shear-layer mean-velocity profiles: ——, $0.5(1+\tanh\eta)$; ●, $x/D = 1$; ■, 2; △, 3.5.

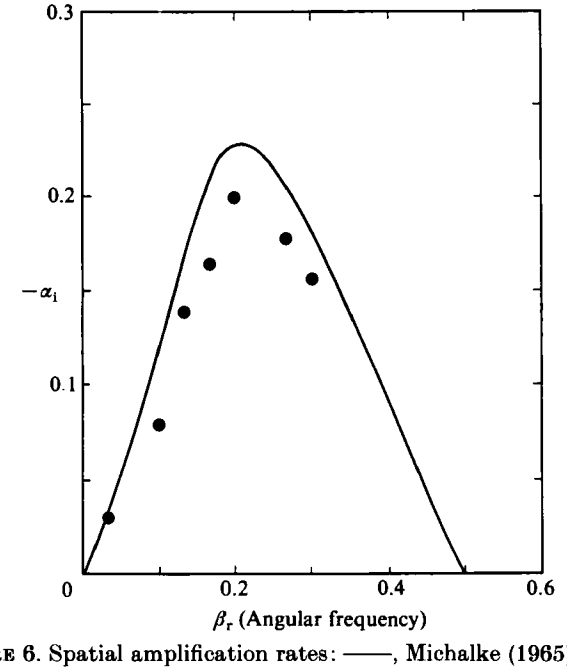

FIGURE 6. Spatial amplification rates: ——, Michalke (1965) theory.

Similar 'rules' for the nonlinear interaction of fluctuations have been put forward by Sato (1970) and Sato & Saito (1975, 1978) in their studies of the transition of a two-dimensional wake. Their work also demonstrated the production of harmonics as well as sum and difference modes. However, studies in wakes have demonstrated the absence of subharmonics, which Miksad (1972) notes as a definite feature of nonlinear free-shear-layer instability. Indeed, Winant & Browand (1974) demonstrate that mixing-layer growth is governed by the pairing of vortical structures, and Ho & Huang (1982) suggest that the location where merging vortices align coincides with the position where the subharmonic reaches its peak amplitude.

For the jet considered here one would expect that the nonlinear interaction of

fluctuations would occur primarily between the modes at 1230 Hz, 1094 Hz and 800 Hz. These three modes dominate the initial jet-shear-layer spectra and have similar amplitudes. Indeed, one would expect the 1230 Hz and 1094 Hz interaction to be especially effective. In the spectrum for $x/D = 3$, the spectral modes near $f_1 \approx 1094$ Hz and $f_2 \approx 1230$ Hz have reached saturation and are in the process of decay. Associated with this decay is the growth of subharmonic components, the one centred near 605 Hz being especially prominent. Much more high-frequency fluctuation energy is also present, and this is directly related to the summation mode (f_1+f_2) and the harmonics $2f_2$ and $2f_1$, as is evidenced from the broad peaks in figure 4(*b*) (showing the $x/D = 3$ shear-layer spectrum on an expanded frequency scale). The difference mode (f_2-f_1) is also present, resulting in a peak near 136 Hz. The spectral measurements of Miksad (1973) also showed strong (f_1+f_2), (f_2-f_1) and $2f_2$ modes.

Other modes present at $x/D = 3$ may be explained in terms of interactions between modes $f_2 \approx 1230$ Hz, $f_1 \approx 1100$ Hz and the mode which will be designated $f_0 \approx 800$ Hz. For example, the relatively large mode near 434 Hz most likely corresponds to the difference mode (f_2-f_0). Similarly, the mode near 307 Hz has two potential sources; the difference mode (f_1-f_0) and/or the subharmonic of the newly created peak at 600 Hz (i.e. $\frac{1}{2}f_2$). Higher-frequency modes corresponding to (f_0+f_1), (f_0+f_2), and harmonics of f_1 and f_0 are also present (see figure 4*b*). In interpreting the above results allowance should be made for some slight spectral shifting (typically less than 8 Hz) caused by possible small differences in the lateral positioning of the probe in the thin jet shear layer at successive x/D stations.

The spectrum at $x/D = 4$ (figure 7) shows the decay of the mode near 800 Hz. The spectrum also shows a general redistribution or 'smoothing' which greatly enhances the energy content at low frequencies. This smoothing is due to the many interactions that must occur between the newly created lower-frequency spectral models described above. Sato (1970) has suggested the term 'amplification of randomness' to describe the mechanism by which this spectral smoothing occurs. An example of this phenomenon is the interaction of two spectral modes f_1 and f_2 to form the difference mode (f_2-f_1). Suppose now that the frequency f_2 changes by Δf due to some inherent small randomness, resulting in a percentage change of $100\Delta f/f_2$. The difference mode then changes by $100\Delta f/(f_2-f_1)$. Since the spectral-mode interaction is most efficient for f_1 and f_2 close together, the percentage increase in randomization is apparent. In fact, one may imagine a process by which the effect 'cascades' across the frequency domain owing to repeated interactions.

Of interest in the $x/D = 4$ spectrum is the renewed growth of the mode near 1200 Hz and a continued increase in the energy content at higher frequencies. This 'secondary' or renewed growth of a spectral component also occurs for the mode near 800 Hz but farther downstream, as is apparent from a comparison of the spectra at $x/D = 4$ and 5 (figure 7). Thus the reappearance of these modes occurs in the same order in which they originally decayed. However, the reason for their secondary renewed growth is not certain from these data. One possibility is that these modes are acting as harmonic components of associated newly created subharmonics.

Figure 7 shows that with increasing downstream distance the 'humps' in the shear-layer spectra smooth and a continuous spectrum gradually forms; evidence of the increased randomization of velocity fluctuations in the jet shear layer leading to turbulence. Indeed, it is this randomization in phase and amplitude of the velocity fluctuations in the shear layer that makes discerning evidence of large-scale structural patterns so difficult.

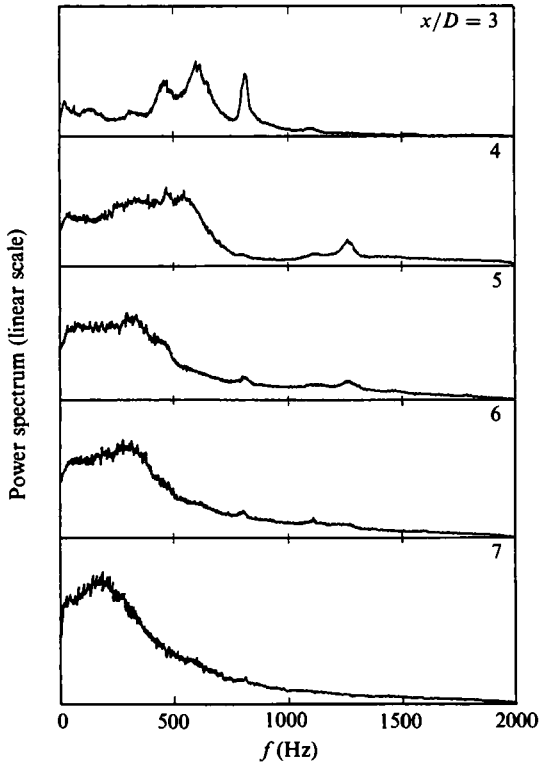

FIGURE 7. Shear-layer spectral development, $3 \leqslant x/D \leqslant 7$.

This problem was addressed by Lau, Fisher & Fuchs (1972), who studied fluctuating quantities in the potential core and near-exit entrainment regions of an axisymmetric jet. They assumed that fluctuations in these regions resulted from events which occurred in the mixing region and were convected downstream. Measurements made in these non-turbulent regions were then used to make inferences about the coherent structures in the mixing region. The rationale for doing this was that, if fluctuations in the non-turbulent regions were manifestations of the field having its origin in the mixing region, then more information could be obtained about the hidden structures by taking data in the vicinity, where the effects of the coherent field were not washed out by the small-scale turbulence.

The potential core of the planar jet extends to approximately $x/D = 6$. The intensity profiles in figure 3 show that velocity fluctuations originate in the shear layers that border the potential core. The irrotational fluid forming the potential core would then be expected to experience fluctuations induced by the activity in the shear layers. In the spirit of Lau, Fisher & Fuchs (1972) one would expect that the longitudinal fluctuation spectra obtained on the jet centreline in this region would mirror the data obtained for the shear layer (aside from some spectral shifting due to different phase velocities) but with less of the background turbulence that otherwise obscures the principal modes.

The initial development of the centreline spectra is shown in figure 8. Comparison of the centreline and shear-layer spectra reveals several modes common to each. As expected, the initial amplitudes of all the centreline spectral modes are quite reduced from their shear-layer counterparts (though this disparity decreases with downstream

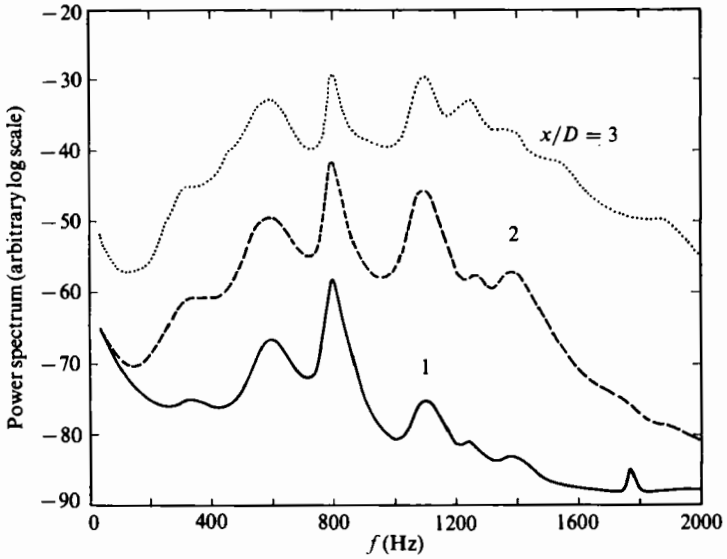

FIGURE 8. Initial centreline spectra.

distance). An important difference to note is that the relative amplitudes among the centreline spectral modes are quite different from what occurs in the shear layer. In particular, the initially most amplified shear-layer mode near 1230 Hz is not present on the centreline. At the same time a centreline mode near 600 Hz exhibits amplitudes comparable to the 800 Hz and 1100 Hz centreline modes. A strong subharmonic shear-layer mode near 600 Hz was noted to form near $x/D = 3$. This suggests the possibility of an upstream influence on the jet core by that shear-layer mode.

The centreline spectral peaks are 'cleaner', since many of the random fluctuations originating in the shear layer are absent; they show clearly the dominance of the subharmonic mode at $f \approx 600$ Hz to nearly the end of the potential core. Of particular interest is the sequence of figure 9 showing a gradual halving of the dominant centreline spectral frequency. The formation of this new mode is associated with the merging of the shear layers near the end of the potential core.

It must be noted that the previous discussion regarding the nonlinear interaction of modes that lead to planar-jet transition is to a certain extent speculative in nature. Power-spectral measurements of the type made in this study can only provide clues and suggestions concerning the nature of newly generated spectral components. A higher-order spectral measurement known as the bispectrum provides the capability of determining whether a particular spectral mode occurs owing to nonlinear interaction or is an unstable mode of the basic flow (see Miksad *et al.* 1981). This technique has recently come to prominence in studies of the nonlinear transition of free shear flows (e.g. Knisely & Rockwell 1982; Miksad *et al.* 1982; Monkewitz 1983; and Miksad *et al.* 1983). It is desirable that future research into planar-jet transition employs such methods in order to quantify fully the modal interactions leading to turbulence.

Beyond x/D of about 8 the natural jet spectra on both the centreline and shear layer ($y/b = 1.0$) are broadband (indicating the presence of turbulent flow conditions), while also possessing a maximum amplitude at some frequency which will be designated f_p (an example is shown in figure 10*a*). A plot of these peak frequencies for the centreline and shear-layer spectra as functions of downstream distance is

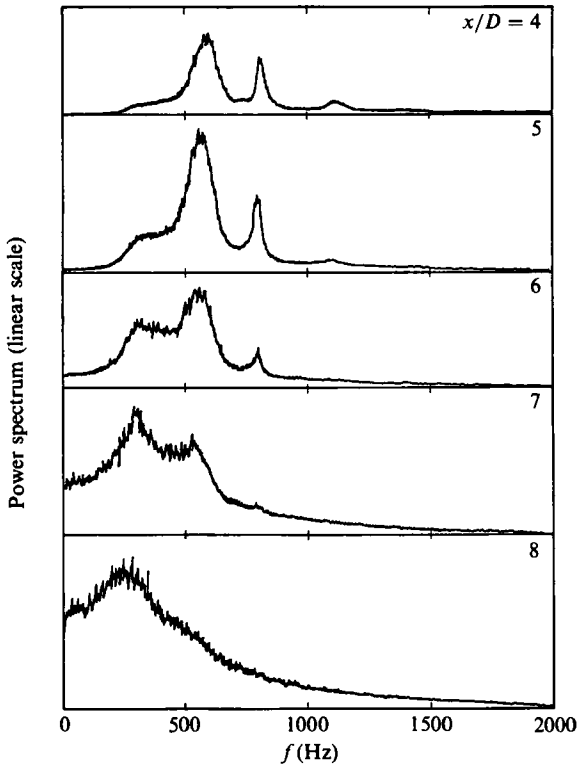

FIGURE 9. Centreline spectral development.

presented in figure 10(*b*). The spectral peak frequencies are non-dimensionalized by the slot width D and exit velocity U_0. It may be observed from this plot that initially

$$f_{\mathrm{p,CL}} \approx 2f_{\mathrm{p,SL}}, \tag{3}$$

while further downstream the condition

$$f_{\mathrm{p,CL}} \approx f_{\mathrm{p,SL}} \tag{4}$$

is gradually approached.

It is informative to compare these data on a wavenumber basis. The wavenumbers k_{SL} and k_{CL} are defined as

$$k_{\mathrm{SL}} = \frac{2\pi f_{\mathrm{p,SL}}}{C_{\mathrm{SL}}}, \quad k_{\mathrm{CL}} = \frac{2\pi f_{\mathrm{p,CL}}}{C_{\mathrm{CL}}}, \tag{5}$$

where C is a local structural convective velocity. Several researchers have investigated the convective velocities in the near-exit region of jets, as reported by Goldschmidt, Young & Ott (1981). Based on that work one can approximate, for $y/b \leqslant 1$,

$$C_{\mathrm{SL}} \approx C_{\mathrm{CL}}; \tag{6}$$

hence,

$$k_{\mathrm{SL}} \approx \tfrac{1}{2}k_{\mathrm{CL}}, \tag{7}$$

and if λ_{s} is interpreted as a local structural wavelength that characterizes the large-scale flow structures then figure 10(*b*) suggests that just beyond the potential core

$$\lambda_{\mathrm{s,CL}} \approx \tfrac{1}{2}\lambda_{\mathrm{s,SL}}, \tag{8}$$

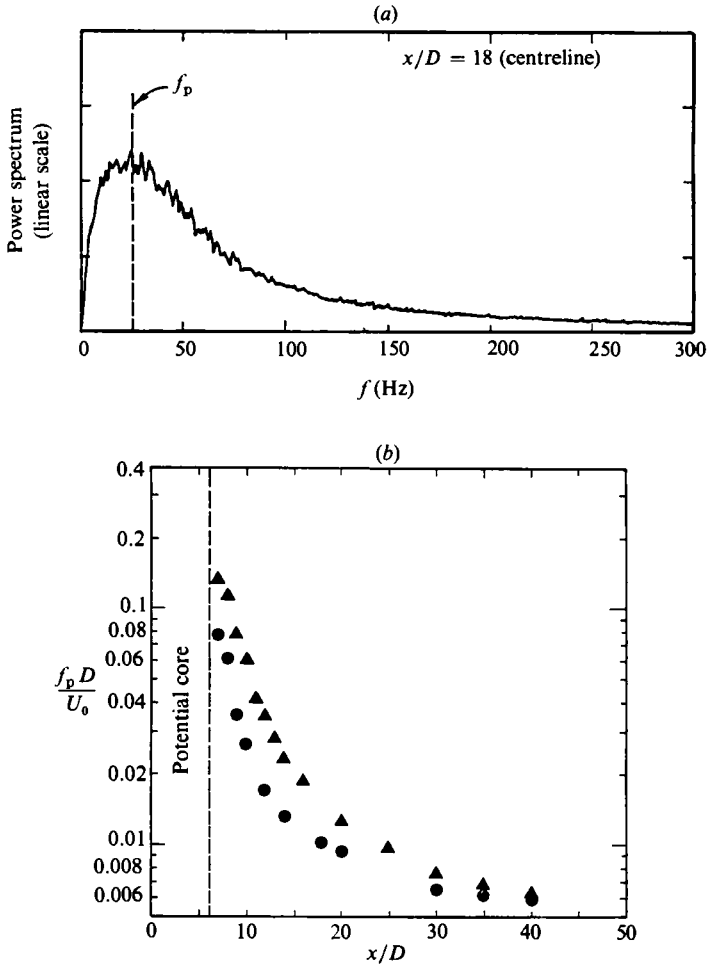

FIGURE 10. (*a*) Definition of peak spectral frequency f_p. (*b*) Peak spectral frequencies on centreline (▲) and shear layer (●).

whereas, sufficiently downstream,

$$\lambda_{s,SL} \approx \lambda_{s,CL}. \tag{9}$$

These observations will be examined further, based on the lateral correlation measurements which will be presented next.

3.2. *Lateral space–time correlations*

Space–time correlation measurements were performed on longitudinal velocity-fluctuation probe signals obtained at $y/b = 1$ and $y/b = -1$ for selected x/D stations, to provide additional information concerning structural patterns in the jet. In particular, information concerning the frequency of the correlation function oscillations f_c and phase angle ϕ between the fluctuations on opposite sides of the jet was sought. The correlation function $R_u(\Delta y, \tau)$ is given by

$$R_u(\Delta y, \tau) = \overline{u(x, y = b, z, t)\, u(x, y = -b, z, t+\tau)}, \tag{10}$$

where the overbar denotes a time average.

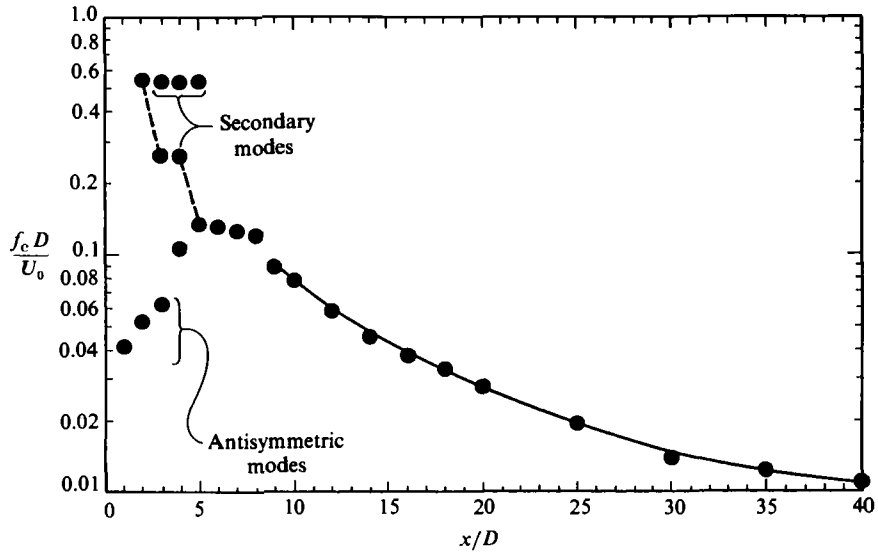

FIGURE 11. Correlation-function frequencies: ——, $f_c D/U_0 = 2.43(x/D)^{-1.5}$.

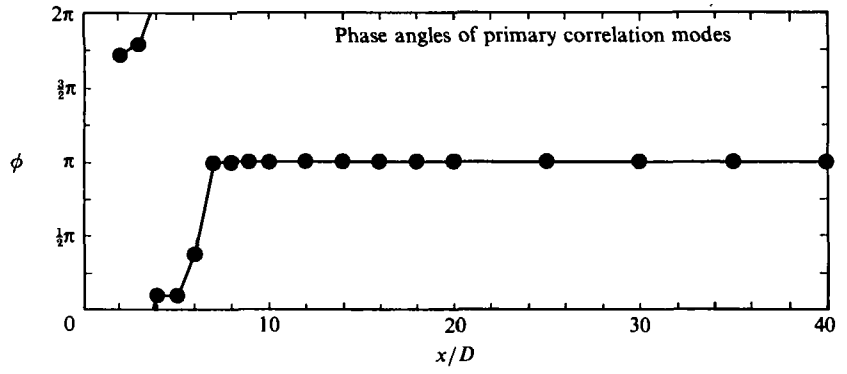

FIGURE 12. Velocity fluctuation phase angles.

The probe separation used in the lateral space–time correlation measurements is large compared to the lengthscales of the fine-grained turbulent-velocity fluctuations. Hence the smaller scales should show little correlation compared to the large-scale fluctuations (structural wavelength, $\lambda_s \approx b$). It is expected that correlation of anemometer signals over a lateral separation of $2b(x/D)$ will show mainly the effects of the large-scale flow structure.

The correlation-function frequencies f_c (in non-dimensional form) obtained for the jet are presented in figure 11. Corresponding phase data are shown in figure 12, where the experimental uncertainty is less than 0.40 rad. It may be noted that in the initial region the correlation function exhibits frequencies similar to those that characterized the dominant natural spectral modes ($fD/U_0 \simeq 0.5$, 0.25 and 0.125). The correlation frequency also shows the rather sudden halving of frequency (i.e. subharmonic formation) that characterized the spectral development. It may be noted from the phase plot that the dominant structures of the initial region show small phase angles and are, to a good approximation, symmetrically distributed with respect to the jet

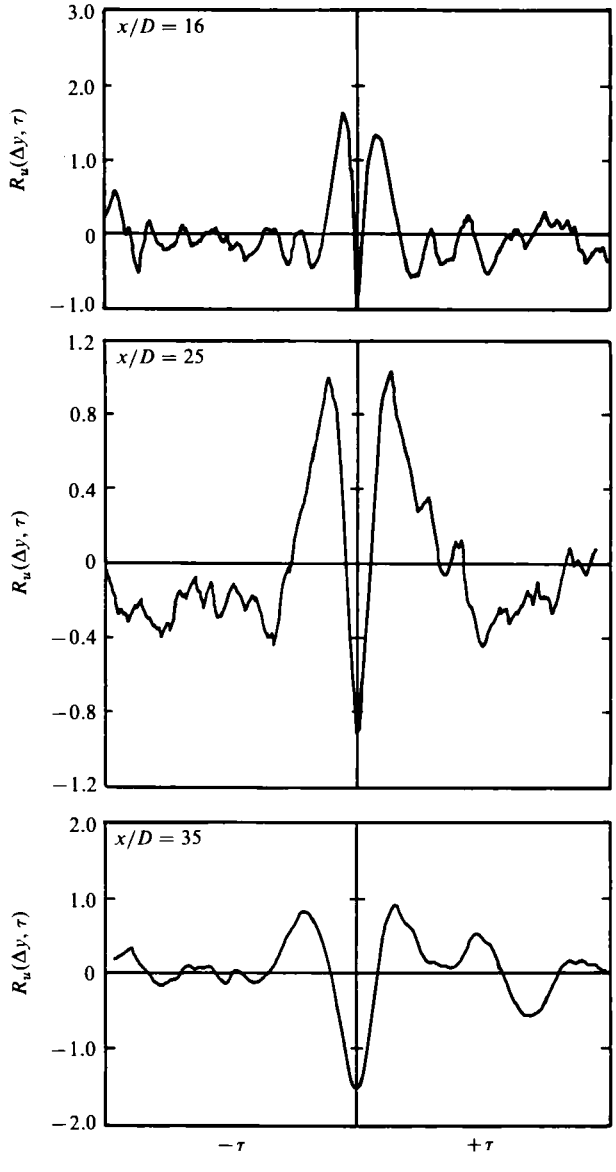

FIGURE 13. Lateral space–time correlations obtained in the similarity region.

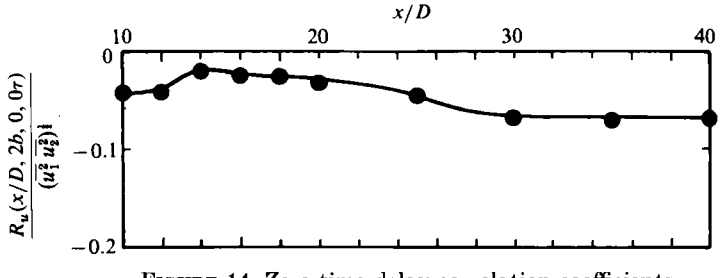

FIGURE 14. Zero time-delay correlation coefficients.

centreline. There is a rather sudden jump to an antisymmetric arrangement at $x/D = 7$. This corresponds to the merging of the two shear layers at the end of the potential core. The switch from a symmetric to an antisymmetric pattern was also observed by Antonia *et al.* (1983) to occur downstream of shear-layer merging but upstream of the onset of self-preservation. Associated with shear-layer merging is a second halving of the correlation-function frequency (which has also been noted in the spectral sequence of figure 9). Though the switch from a symmetric to an antisymmetric array could be explained simply by streamwise shifting of existing structures with respect to each other, the observed halving of the correlation frequency can not. Simple shifting of the structures to form an antisymmetric arrangement would leave the correlation-function frequency unchanged, while the centreline spectral passage frequency should be doubled. In fact this does not occur. The centreline spectral frequency is halved, as is the correlation-function frequency. This could only occur owing to an amalgamation or destruction of certain participating structures.

The correlations obtained beyond the end of the potential core ($x/D \geqslant 8$) are all similar in form to those in figure 13. It must be noted that the correlations shown have not been normalized, so the magnitude on the ordinate is in a certain sense arbitrary, though consistent among the three plots shown. Each correlation is characterized by strong negative correlation at zero time delay ($\tau = 0$), which suggests an antisymmetric structural arrangement in the flow, confirmed in figure 12. It may also be noted that at each of these downstream stations the amplitude of the correlation-function oscillations decays with increasing time delay. This is due to the increasing randomization that occurs in this region (the energy spectra are broadband). As an indication of the degree of asymmetry existing in the flow and to supplement the information provided in the correlation-function plots, figure 14 shows the normalized zero-time-delay correlation coefficient as a function of x/D.

The passage frequencies of structures decrease in a continuous fashion satisfying, for $x/D > 9$, the relation

$$\frac{f_c D}{U_0} = 2.43\left(\frac{x}{D}\right)^{-1.5}. \tag{11}$$

The $(x/D)^{-1.5}$ variation satisfies the requirements for similarity of the structural length and velocity scales. The frequency f_c, when non-dimensionalized by the U_M and b, is a constant,

$$\frac{f_c b}{U_M} \simeq 0.11. \tag{12}$$

Cervantes (1978), Oler (1980) and Oler & Goldschmidt (1982) have also found the same value in separate test set-ups, suggesting the universality of the above value for plane jets. That the measured correlation or 'flapping' frequencies satisfy the requirements for global similarity is important. This further strengthens the assumption that the correlation oscillations are due to the large-scale structures of the flow. If the entire jet flapped (as a flag does) then one would expect travelling-wave behaviour which would not satisfy mean-flow similarity requirements.

Consider a flow possessing pseudo-periodic velocity fluctuations. These fluctuations may be thought of as arising from the progression of a sequence of large-scale flow structures convected past fixed probes situated on opposite sides of the jet. The randomness in the frequency of the fluctuations is due then to a random distribution in the longitudinal spatial separation of the structures. Thus we consider sinusoidal

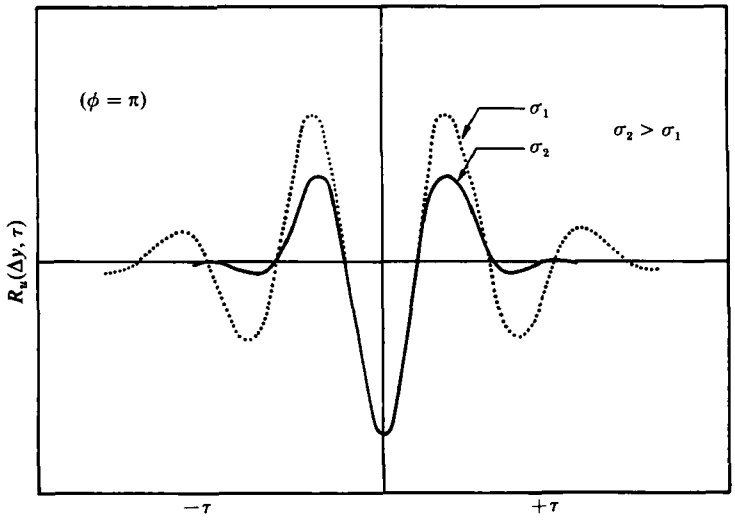

FIGURE 15. Calculated lateral correlation functions.

velocity fluctuations with an angular frequency ω, a normally distributed random variable with mean value ω_0 and standard deviation σ. The velocity fluctuations can then be represented by

$$\left.\begin{aligned} u_1 &= A_1 \sin \omega t, \\ u_2 &= A_2 \sin [\omega(t+\tau)+\phi], \end{aligned}\right\} \tag{13}$$

where A_i = amplitude and ϕ = phase angle of u_2 with respect to u_1. The joint probability density is, then,

$$P(\omega, t) = \frac{\omega}{(2\pi)^{\frac{3}{2}}\sigma} \exp\left[-\frac{(\omega-\omega_0)^2}{2\sigma^2}\right], \tag{14}$$

while the correlation function becomes

$$R(\tau) = \int_{\omega_0-\Delta\omega}^{\omega_0+\Delta\omega} \frac{A_1 A_2}{\sigma(2\pi)^{\frac{3}{2}}} \exp\left[-\frac{(\omega-\omega_0)^2}{2\sigma^2}\right]\left[\cos\phi \int_0^{2\pi/\omega} \sin\omega t \sin[\omega t+\omega\tau]\,dt + \sin\phi \int_0^{2\pi/\omega} \sin\omega t \cos[\omega t+\omega\tau]\,dt\right] d\omega, \tag{15}$$

which after integration gives

$$R(\tau) = \tfrac{1}{2}A_1 A_2 \cos(\omega_0\tau+\phi) \exp[-\tfrac{1}{2}\tau^2\sigma^2]. \tag{16}$$

Figure 15 shows (16) for $\phi = \pi$ (antisymmetric patterns) and two values of σ. It very nearly approximates representative measured correlations shown in figure 13.

The oscillatory modes that have been described for the correlation functions obtained prior to the end of the potential core are due to symmetric velocity fluctuations. However, the correlation data also indicate the presence of antisymmetric modes in this initial region. The mean frequencies of the near-exit antisymmetric fluctuations may be seen in figure 11 (along with the symmetric modes). The antisymmetric-mode frequencies are noted to be much lower than the corresponding symmetric-mode frequencies. In addition their mean frequency increases with downstream distance until $x/D = 4$, at which point no antisymmetric mode is noted.

Of significance is the recognition that the passage frequency and phasing of structures beyond the end of the potential core are the same as those of the antisymmetric modes present in the initial region of the jet. This suggests that these antisymmetrically distributed structures may exert an upstream influence on the developing flow. Laufer (1981) has questioned whether such a feedback effect may occur in free jets. Preliminary measurements by Laufer & Monkewitz (1980) in a round jet are encouraging in this respect. They show that the initial shear-layer hot-wire signals exhibit modulation at a frequency corresponding to the downstream vortex passage frequency, similar to the effects reported in Thomas (1983).

Sato (1960) found two types of velocity fluctuations in studies on the transition of a two-dimensional jet. Fluctuations at higher frequencies were noted to be symmetrical with respect to the centreline, while low-frequency modes were antisymmetrical. It was found that the relative intensity of the two modes was highly dependent on the initial mean-velocity distribution. A parabolic-type distribution led to the dominance of the antisymmetric modes. Flat profiles such as that observed in the current study resulted in the dominance of the symmetric mode. Schlichting (1934) demonstrated that the velocity distribution in the inlet region of a laminar two-dimensional channel of length l and width D depends on the parameter $4\nu l/D^2U_{\mathrm{M}}$. Larger values of this parameter correspond to parabolic profiles, while flat profiles occur for smaller values. Sato (1960) found the dominance of symmetric-mode disturbances for $4\nu l/D^2U_{\mathrm{M}} = 0.024$. When this parameter is calculated for the jet used in the current study it is found that $4\nu l/D^2U_{\mathrm{M}} = 0.0007$. Hence the dominance of the symmetric mode in this study is not at all surprising. This is not to say that the antisymmetric modes play no role in the development of the planar jet. It may be noted from figure 11 that the disappearance of the antisymmetric mode is associated with the formation of a symmetric oscillation at approximately twice the frequency at $x/D = 4$. This frequency is, in turn, approximately one-half that of the former symmetric-mode oscillation. This is suggestive of an interaction between these modes to form the structures near the end of the potential core.

The initial dominance of the symmetric mode as observed in this work was also reported by Antonia *et al.* (1983). However, Weir & Bradshaw (1975) reported the dominance of the antisymmetric mode for $x/D < 20$ in their jet. Rockwell & Niccolls (1972) performed flow-visualization studies of the initial structural development of a planar jet and found for a certain range of Reynolds number that the jet cycled randomly between symmetric and antisymmetric modes. The exact cause of the cycling was not known, but initial conditions were suspected. Since all correlation measurements in the current study were based on ensemble averaging it is possible that this sort of 'switching' between modes could lead to the appearance of the secondary antisymmetric correlation modes noted in the initial region.

3.3. *Measurements of the two-dimensionality of structural patterns in the jet*

The basic geometry of the planar-jet flow field suggests that two-dimensionality may be exhibited by the large-scale flow structures. The two-dimensionality of flow patterns in the developing jet was investigated at the selected streamwise distances of $x/D = 4$, 8, 12 and 20. Two-point correlations of the longitudinal velocity fluctuations were performed with hot-wire probes separated in the z-direction (i.e. direction of mean-flow homogeneity) for vertical correlations or in the x- (streamwise) direction for longitudinal correlations. The probes were laterally located at $y/b = 1$ for these measurements.

In order to quantify the extent of two-dimensionality the integral macroscales Λ_z

x/D	$\Lambda_z/b(x/D)$	Λ_z/D	$\Lambda_x/b(x/D)$	Λ_x/D	Λ_z/Λ_x
4	2.69	1.53	0.61	0.35	4.41
8	0.51	0.43	0.91	0.76	0.56
12	0.36	0.49	1.16	1.57	0.31
20	0.35	0.79	0.75	1.69	0.47

TABLE 1. Measured Λ_z and Λ_x macroscales

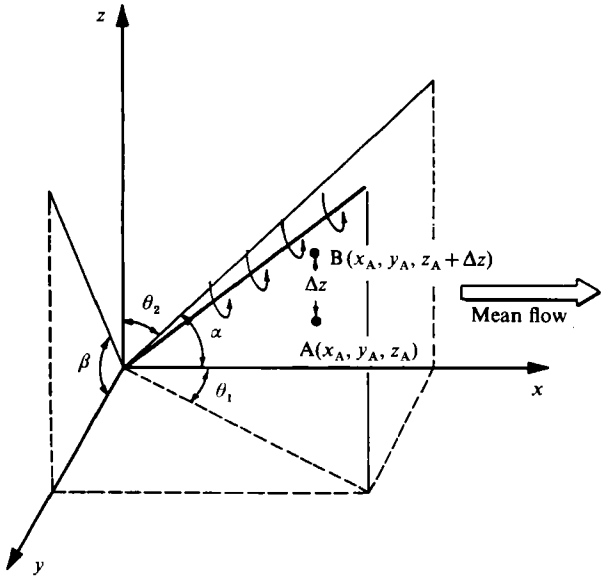

FIGURE 16. Hypothetical two-dimensional structure.

and Λ_x (corresponding to the integrated vertical and longitudinal correlation coefficients respectively) were determined and are presented in table 1. Both the vertical and longitudinal macroscales are presented. Each has been normalized by the local mean-velocity half-width as well as the nozzle width. Of particular interest is the ratio Λ_z/Λ_x, which is expected to provide an indication of the extent of two-dimensionality exhibited by the flow patterns.

Initially there is significant two-dimensionality, as is evidenced by $\Lambda_z/\Lambda_x = 4.4$. This ratio rapidly decreases with downstream distance owing both to a longitudinal macroscale which scales with the mean-velocity half-width and to a genuine reduction in the vertical macroscale. Values at $x/D = 20$ suggest that the flow is not strongly two-dimensional, as Λ_z/Λ_x is only 0.47. This agrees with the results of Oler (1980), who found $\Lambda_z/\Lambda_x = 0.43$, and Everitt & Robins (1978), who found $\Lambda_z/\Lambda_x = 0.49$ (both from measurements in the similarity region).

It must be noted that a small value of Λ_z/Λ_x does not necessarily imply absence of elongated structures in the flow. One may visualize a hypothetical flow structure that possesses a high degree of two-dimensionality and yet is tilted at some arbitrary angle with respect to both the (x, z)- and (y, z)-planes. In addition, one could conceive of a structure that undergoes periodic (wave-like) undulations along its length.

Figure 16 shows a hypothetical, two-dimensional structure located in the flow. The

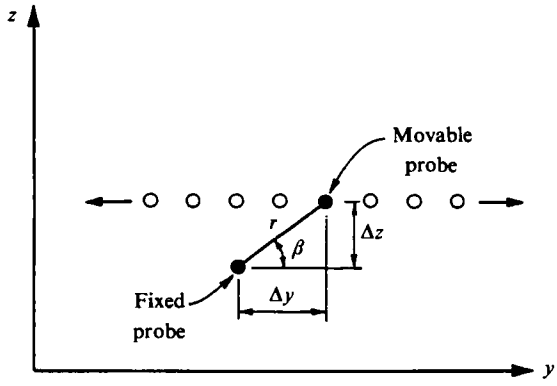

FIGURE 17. Probe arrangement for measurement of lateral inclination of structure. Jet flow is out of the plane of the figure.

line of symmetry of the structure may be characterized by the angles θ_1 and θ_2. These angles may be directly related to projected angles α (in the (x,z)-plane) and β (in the (y,z)-plane). Consider now the two probes at $\mathrm{A} = (x_\mathrm{A}, y_\mathrm{A}, z_\mathrm{A})$ and $\mathrm{B} = (x_\mathrm{A}, y_\mathrm{A}, z_\mathrm{A} + \Delta z)$. Due to the structural inclination, the structure will pass probe location B before A (though cases may be visualized in which the opposite is certainly true).

In order to account for any inclination of the structure in the (x,z)-plane, application of the time-delay feature of the two-point space–time correlation can be made. It may be expected that the correlation function $R_u(0,0,\Delta z,\tau)$ will show a maximum at some time delay τ_M corresponding to the delay required for the structure to reach point A after traversing probe B. Measured space–time correlations would thus be expected to exhibit shifting in τ corresponding to changes in probe separation Δz if such streamwise-inclined, extended structures are present.

An extensive set of space–time correlations were made at x/D stations of 4, 8, 12 and 20 for several Δz probe separations. No strong evidence was found in any of these measurements to indicate streamwise structural leaning.

An extended two-dimensional structure in the flow could be laterally inclined at some angle β with respect to (x,y)-planes (see figure 16). In order to check for this type of inclination, a special series of correlation tests were performed at x/D stations of 8, 12 and 20. The probe arrangement for these measurements is shown in figure 17. The 'fixed probe' was laterally located at $y/b = 1.0$. A second movable probe was placed Δz above the fixed probe. The lateral separation between the probes is designated Δy. The lateral angle β is then simply $\tan^{-1}(\Delta z/\Delta y)$ and r is $(\Delta z^2 + \Delta y^2)^{\frac{1}{2}}$. The angle β was taken as zero when aligned with the y-axis (i.e. pointing outside the jet) and π when directed toward the jet centreline. The probe separation was typically $\Delta z = 0.318$ cm (0.125 in.), corresponding to roughly $0.8 > \Delta z/b(x/D) > 0.2$ over the streamwise range $8 \leqslant x/D \leqslant 20$. Other vertical separations were tried and were found to give results similar to those that will be reported. It was desired to keep the laterally traversed probe out of the intermittent region of the jet and yet cover a representative range of β. This put an upper limit on the value of $\Delta z/b$ at each streamwise station. For example, at $x/D = 20$ the maximum $\Delta z/b$ tested was 0.25.

The correlation coefficients measured in this manner were observed to have the general form

$$\rho_u(r) \simeq \exp\left[-\frac{kr}{\Lambda_r}\right] \tag{17}$$

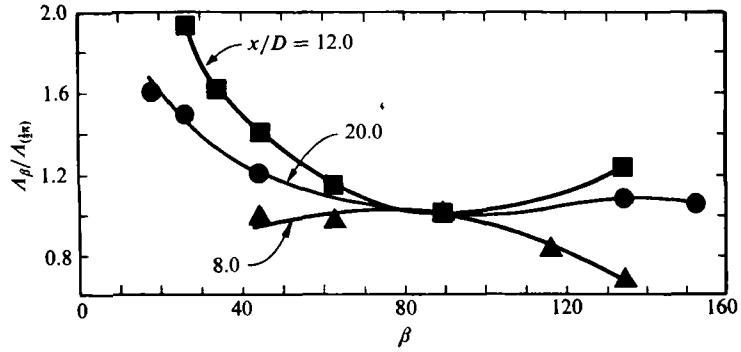

FIGURE 18. Jet $\Lambda_r(\beta)$ macroscales at selected x/D stations.

(but of course only for probe separations r producing positive correlation). In the above expression k is a constant and Λ_r is the macroscale corresponding to the direction of probe separation. Thus we write

$$\frac{\Lambda_r}{k} = \frac{-r}{\ln \rho_u(r)}. \tag{18}$$

The above relation enables the determination of a representative macroscale in the direction of probe separation.

The results of the measurements to detect lateral inclination of flow structures are presented in figure 18. The ordinate is the ratio of the macroscale corresponding to the angle β non-dimensionalized by the macroscale at $\beta = \frac{1}{2}\pi$ (which has been previously termed the vertical macroscale Λ_z and was tabulated in table 1). The abscissa is the lateral inclination angle. (The movable probe would have been on the jet centreline at β values of 148°, 142° and 155° for $x/D = 8$, 12 and 20 respectively.)

The Λ_r macroscales obtained at $x/D = 8$ decline for $\beta > 90°$ and are approximately constant for $\beta < 90°$. The results obtained at $x/D = 12$ are substantially changed. They show a minimum macroscale at $\beta = 90°$ and a substantial increase in the Λ_r values for smaller β. In fact, at $x/D = 12$ the macroscale near $\beta = 30°$ is approximately double the vertical macroscale value. This increase in the value of Λ_r over that at $\beta = \frac{1}{2}\pi$ for large lateral inclination, coupled with the absence of any measurable streamwise inclination of an extended structure, suggests that the loss of z-directed two-dimensionality indicated in table 1 has come about due to a lateral reorientation of the structure. Measurements at $x/D = 20$ indicate the continued presence of the same type of laterally inclined structure. From the data obtained at $x/D = 20$ it appears that the flow structures must be nearly horizontal, for if a maximum Λ_r does occur it is such that $\beta_{\max} < 15°$.

Mumford (1982) performed an experimental study of the structure of large eddies in the fully developed region of a two-dimensional jet. It is interesting to note that a major result of that study was the indication that the large-scale structures in the fully developed region of the flow are roller-like structures with the axes aligned with the direction of mean strain or in the direction of mean-flow homogeneity. This would seem to be in at least qualitative agreement with the measurements now presented.

Detection of the development of nearly horizontal structures in the flow is consistent with the fact that the $R_u(\Delta z, \tau)$ correlations never exhibited any indication of structural leaning in the streamwise direction. Referring to figure 16, it may be noted that time-delay correlations between Δz-separated probes would not be

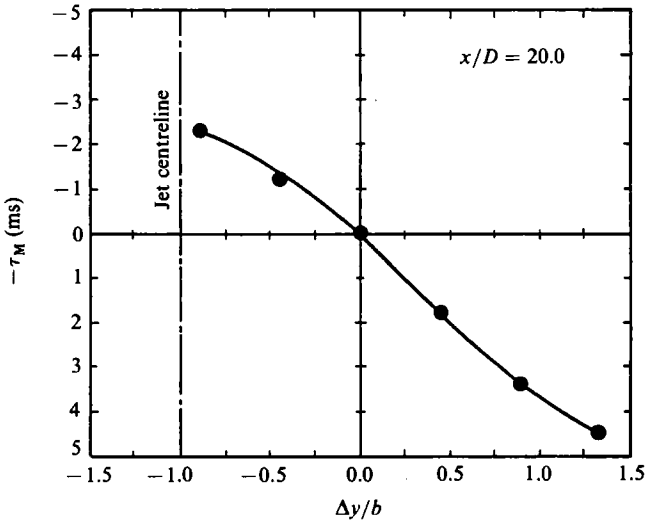

FIGURE 19. Time-delay values for maximum correlation.

expected to detect even substantial existing streamwise inclination of structures that are nearly horizontal (i.e. $\beta \approx 0$).

Experiments were performed in order to detect any possible streamwise inclination of the suspected roller-like structures. These limited measurements were made at $x/D = 20$, since the Λ_τ measurements suggested that the envisioned structural development was more nearly complete at this station. The results are presented in figure 19. The time delay for maximum correlation may be related to the streamwise inclination of the structure θ_1 by the relation

$$\theta_1 = 90° + \tan^{-1}\left\{\frac{\tau_M U_c}{\Delta y}\right\}, \tag{19}$$

where U_c is a local convective velocity of the large-scale structure and $\Delta z = 0$.

The time delay varies approximately linearly over a limited range of y/b. The deviation from a linear variation of τ_M with Δy may originate from apparent streamwise bending of the roller-like structure or from a lateral variation of the convective velocity (or both). Goldschmidt *et al.* (1981) have performed a study of convective velocities in a natural plane turbulent jet. This work demonstrated the frequency dependence of measured convective velocities. For the lower-frequency components the variation across the flow is small, though there is a trend for the convective velocity at any particular wavenumber to increase for $y/b > 1.0$. Most likely then, the observed functional variation of τ_M with Δy results primarily from a genuine apparent inclination of the structure in the mean-flow direction (though some effects of convective-velocity variation across the flow are likely to be present). If it is assumed that the convective velocity for these cases is approximately constant across the flow and $U_c \approx 0.50 U_M$ (as indicated by Goldschmidt *et al.* (1981) for the largest eddies) the inclination angle θ_1 is found to be $\theta_1 = 130°$. Though there exists some uncertainty with regard to the choice of U_c, it is very unlikely that $U_c > U_M$ for the large-scale structures. For $U_c = U_M$ one obtains $\theta_1 = 152°$, which may be considered an upper limit. These results compare well with those of Mumford (1982), who reported $\theta_1 = 135°$ based upon correlation measurements and $\theta_1 = 140° \pm 15°$

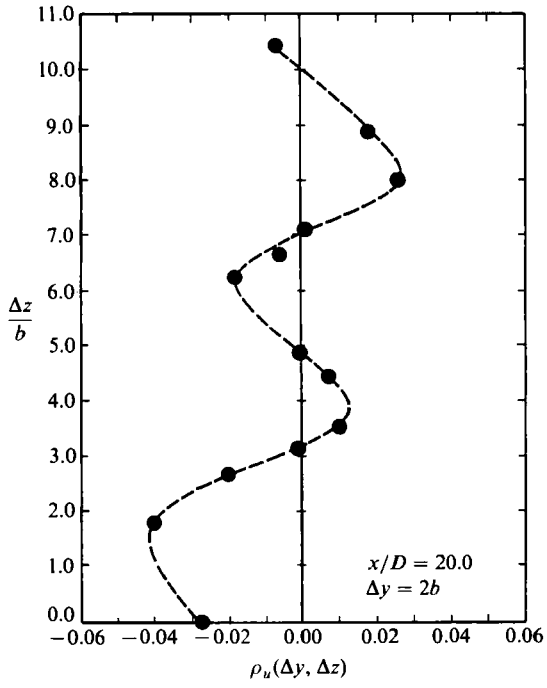

FIGURE 20. $\rho_u(\Delta y, \Delta z)$ at $x/D = 20$.

based on pattern-recognition techniques. It would appear then that the laterally inclined structures are approximately aligned with the direction of mean shear. These data would also suggest a reduction of the structural inclination angle θ_1 towards the jet centreline.

The presence of structures possessing high lateral inclinations raises questions concerning the distribution of such structures in the direction of mean-flow homogeneity. The detection of extended, nearly horizontal structures in the flow suggests that the planar jet is not structurally two-dimensional in the direction of mean-flow homogeneity. The apparent presence of inclined structures would seem to imply the possibility of separate structural patterns existing in separate (x, y)-planes. In particular, how can the apparent structural inhomogeneity in z be reconciled with measurements which show that the local mean velocity is independent of z?

It may be recalled that the lateral correlation measurements discussed earlier provided a means of determining the phase relationship between the large-scale structures on opposite sides of the jet centreline. Such measurements showed the eventual formation of an antisymmetric structural distribution beyond the potential core. For those measurements the probes were only separated laterally ($\Delta y = 2b$) so that the measurements provide phase data for structures located on opposite sides of the jet but in the same (x, y)-plane. These measurements were repeated at $x/D = 20$ with the probes also separated vertically by Δz as well as laterally.

Such measurements provide an important test regarding the existence of separate structural patterns in successive (x, y)-planes. It has been demonstrated that $\rho_u(\Delta y = 2b, \Delta z, \tau = 0)$ exhibits negative correlation for $\Delta z = 0$ (i.e. antisymmetric array). Results of the $\rho_u(\Delta y = 2b, \Delta z, \tau = 0)$ measurements performed at $x/D = 20$ are shown in figure 20 and demonstrate an oscillation of the correlation coefficient

with Δz. Increasing Δz leads to positive correlation followed, in turn, by the return of negative correlation and so on. These data suggest that the structural pattern associated with each (x, y)-plane is streamwise shifted by one-half wavelength with respect to patterns above and below it.

The oscillatory behaviour of these correlation coefficients would thus seem to add strong support for the supposition put forward concerning structural patterns in the turbulent plane jet. The z-directed wavelength of the correlation-cofficient oscillations may be noted from the figure to be $\lambda_{\Delta z}/b = 4.5 \pm 0.5$. When expressed in terms of the separation of the flow-field-confining plates h it is found that $h/\lambda_{\Delta z} \approx 5$. Further, since each correlation-cofficient wavelength must bound two 'layers' of structure, it is seen that the flow may contain up to 10 layers of separate roller-like structures. This may explain the apparent z-directed mean-flow homogeneity of traditional two-dimensional turbulent jets.

4. Discussion of jet-development aspects

The data presented suggest the following characteristics.

4.1. *Initial jet development*

Both symmetric and antisymmetric fluctuations exist in the initial region of the natural jet. The antisymmetric modes are at frequencies substantially lower than the symmetric modes and are localized in the shear layers near the jet-nozzle exit. The frequency and phase of these fluctuations match those of flow structures just beyond the potential core, suggesting the possibility of resonant forcing of the nascent shear layers. The initial shear-layer antisymmetric modes are dominant very near the nozzle exit and gradually disappear with increasing downstream distance; none is noted for $x/D > 3$–4.

Evidence suggests that these modes interact with symmetric shear-layer fluctuations (through modulation effects) to influence subsequent spectral development. However, symmetric jet shear-layer modes appear to play the dominant role in jet shear-layer structural development. Symmetric oscillatory modes are initially present in the nascent jet shear layers ($y/b = 1$) at small amplitude, and grow with downstream distance in accordance with linearized-stability-theory predictions for spatially amplified disturbances. These modes could, in general, originate from a number of disturbance sources external to the flow, or may simply be naturally occurring disturbance modes characteristic of the unconditional free-shear-layer instability. The measurements reported were performed in an extremely quiet, vibration-free environment, so that it would seem that the latter case is most likely.

Nonlinear transition effects become apparent for $x/D > 2$. These effects are most likely associated with the roll-up (formation) of vortical shear-layer flow structures of the type visualized by Rockwell & Niccolls (1972) in planar-water-jet development. The nonlinear interaction effects (between fluctuation modes) that are observed directly parallel the published results of Miksad (1972) involving the nonlinear transition of two-dimensional free shear layers. Spectral and correlation measurements indicate the formation of jet-shear-layer structures at a frequency corresponding to the most amplified initial symmetric disturbance mode (≈ 1230 Hz). Formation of a dominant subharmonic mode near 600 Hz occurs rather suddenly by $x/D = 3$, suggesting a shear-layer pairing event. The resulting subharmonic mode is symmetric and becomes the dominant structural feature of the flow prior to the end of the potential core (at $x/D \approx 6$). A number of difference modes due to interactions

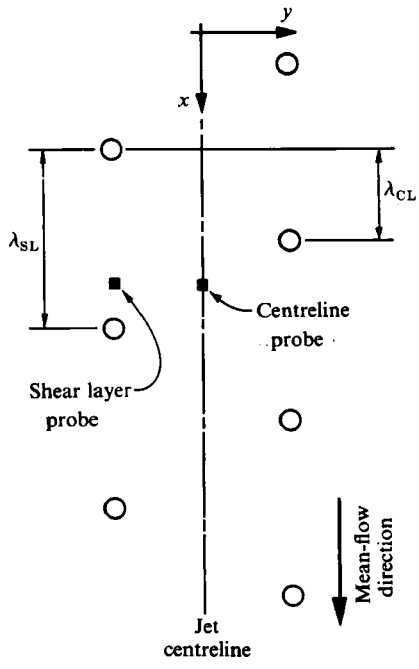

FIGURE 21. Antisymmetric array of flow structures such that $\lambda_{SL} \approx 2\lambda_{CL}$.

between shear-layer symmetric fluctuations at 800 Hz, 1100 Hz and 1230 Hz further enhance the broadband development of the low-frequency spectral range. Spectral measurements indicate, however, that the subharmonic mode near 600 Hz becomes the dominant dynamical feature, overshadowing other difference modes and possibly suppressing subsequent subharmonic formation by the other primary-disturbance modes noted above.

The natural jet shear-layer subharmonic-related structure exhibits significant two-dimensionality. This is evidenced by the fact that the z-directional integral scales are significantly larger than the corresponding streamwise scales. In addition, maximum correlation between the Δz-separated probes situated in the jet shear layer is always found to occur at zero time delay.

The developing jet shear layers (and the associated flow structures) meet near $x/D = 6$. A well-documented halving of the characteristic structural frequency is associated with this merging of the shear layers at the end of the potential core; this event may occur somewhat gradually over a streamwise distance of approximately $2D$–$3D$. The lateral correlation measurements indicate a rather sudden shift to an antisymmetric structural arrangement corresponding to this shear-layer merger. However, the frequency halving cannot be explained merely in terms of phase shifting by one-half wavelength the structural array on one side of the jet with respect to the other side; structural amalgamation or destruction must occur here to produce the observed frequency halving. The shear-layer merging event leads both to the formation of an antisymmetric structural array and a substantial loss in two-dimensionality of the participating structures in the direction of mean-flow homogeneity.

Downstream of the location of jet-shear-layer merging the lateral correlations indicate the continued presence of an antisymmetric structural arrangement. The

broadband shear layer and centreline spectra possess maximum amplitudes at frequencies $f_{p,SL}$ and $f_{p,CL}$ respectively. The associated local structural wavelengths in the shear layer and centreline were related by (8):

$$\lambda_{CL} \approx \tfrac{1}{2}\lambda_{SL}.$$

This relationship was found to apply over a limited distance beyond the location of shear-layer merging ($6 \leqslant x/D \leqslant 12$). Figure 21 shows that the above relationship is expected for an antisymmetric array of flow structures emerging beyond the potential core. Since the centreline probe is equally influenced by the velocity fields from structures on either side of the jet, it will 'see' a wavelength λ_s that is one one-half the shear-layer value. Naturally this will occur only for an antisymmetric structural distribution.

4.2. *Subsequent jet development*

The antisymmetric structural arrangement is maintained well into the similarity region of the flow. The correlation-function frequencies obtained beyond the jet potential core are approximately equal to the shear-layer peak spectral frequencies and obey the global similarity requirements for the flow. In particular it is found that $f_c b/U_M = \text{constant} = 0.11$ for $x/D > 9$. This provides strong support for the supposition that the correlation-function oscillations are due to large-scale flow structures. Further support for a structural interpretation of these measurements stems from the ability of the derived model correlation function to duplicate many of the features of the actual correlations.

The maximum shear-layer and centreline spectral frequencies asymptotically approach each other with increasing downstream distance. It follows then that farther downstream the condition

$$\lambda_{CL} \approx \lambda_{SL}$$

is gradually approached ((9)) even though the structural arrangement in the flow remains antisymmetric. Figure 22 gives one possible physical explanation of this result. The vortical flow structures will grow with downstream distance, scaling with b. Along with this growth the realm of influence of the velocity field associated with the structure also grows. Hence the disparity in the associated structural wavelength 'seen' by a centreline probe compared with that seen by a shear-layer probe would be expected to decrease, as was shown in figure 10(*b*).

The structures sketched in figures 21 and 22 resemble a Kármán-vortex-street type of arrangement. Such a structural arrangement would be expected to show a marked degree of z-directed two-dimensionality. Experimental results show that this is not the case, as evidenced by the small values of Λ_z/Λ_x beyond the potential core (even though a model based on such structures can predict many characteristics, as noted by Oler 1980). Correlation-based searches for z-directed two-dimensionality in the developing region incorporating time delay to allow for streamwise structural inclination reveal no evidence of streamwise tilting of an extended structure. However, correlations between laterally separated probes (on the same side of the jet centreline) do indicate the presence of an extended structure of high lateral inclination. Recall that those structures have been loosely described as roller-like. Figure 23 shows that this type of structure will also satisfactorily explain the $\lambda_{SL} \approx \lambda_{CL}$ trend indicated from the spectral measurements. This figure demonstrates that the effective wavelength 'seen' by the two probes is equivalent simply because of the high lateral inclination. Further, significant z-directed two-dimensionality is

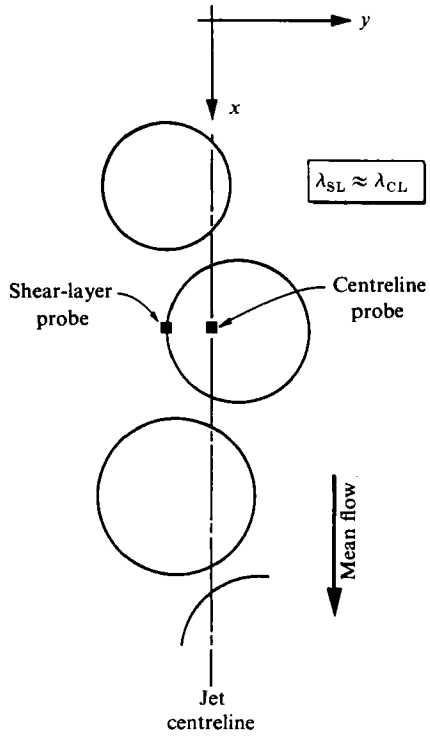

FIGURE 22. Antisymmetric array of flow structures such that $\lambda_{SL} \approx \lambda_{CL}$.

obviously not required by such a structure since there is no structural homogeneity in z. The change in λ_{CL} from a value of $\frac{1}{2}\lambda_{SL}$ near $x/D = 7$ to λ_{SL} at large x/D may then be thought of as arising from a lateral re-orientation of the initially z-directed two-dimensional structures shown in figure 21 to form the laterally inclined roller patterns shown in figure 23.

The measurements presenting time delay for maximum correlation as a function of lateral probe separation suggest that the axis of the inclined structures is aligned approximately with the direction of mean shear. This is not surprising as a number of authors (Tennekes & Lumley 1972; Townsend 1956) note that the ability of an eddy structure to maintain its identity depends on its ability to extract energy efficiently from the mean flow. Such structures are typically vortices whose principal axes are aligned with the mean strain rate. Such an orientation enhances energy transfer through the familiar mechanism of vortex stretching.

There are apparent disparities in the form that the large-scale structural pattern takes in the similarity region, as indicated by the various measurements presented. The lateral correlation and spectral measurements are in support of a Kármán-vortex-street arrangement with passage frequency $f_c b/U_M = 0.11$, as indicated in figure 22. The correlation measurements suggesting structures possessing high lateral inclination are also consistent with the spectral measurements (as indicated in figure 23) and are in agreement with the results of Mumford (1982). However, the requirement of conservation of vorticity at the jet centreline makes it difficult to suppose a roller arrangement with primary circulation component in (x, z)-planes which will also satisfy observations concerning the existence of an antisymmetric pattern in the flow. Obviously any structure proposed must be consistent with all

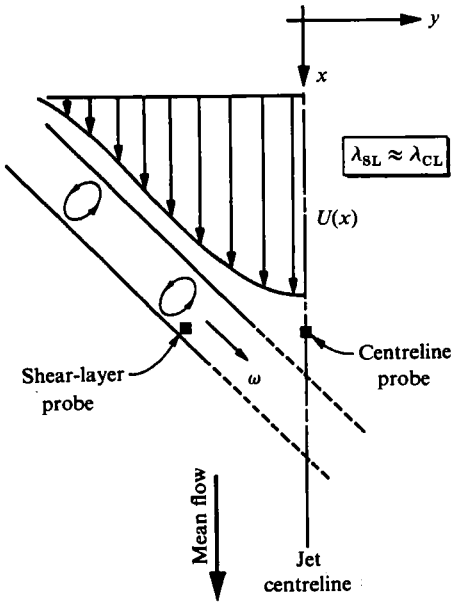

FIGURE 23. Laterally inclined flow structure such that $\lambda_{SL} \approx \lambda_{CL}$.

the experimental results presented. All measurements performed were based on ensemble averaging. It is feasible then that a structure consisting both of rollers with axes aligned in the direction of mean shear and rollers aligned in the direction of mean-flow homogeneity may account for the apparently conflicting observations. Mumford (1982) noted preferred combinations of roller structures in both orientations using pattern-recognition techniques, while Antonia *et al.* (1983) also suggested the possibility that the planar jet supports more than one basic structural form. Averaging over the passage of both z-directed and spanwise rollers may explain the measured Λ_z/Λ_x values of order 0.4 which rule out quasi-two-dimensionality on average. Figure 20, however, would suggest a z-dimension for the structure of approximately $2.3b$, which is about twice Λ_x. Thus concern for the apparent absence of z-directed two-dimensionality for the von Kármán-type eddies may not be completely justified.

It must be emphasized that the measurements detecting laterally inclined structures were not made for $x/D > 20$. In addition, measurements made to determine the streamwise inclinations of such structures were only made at $x/D = 20$. Hence these data on the presence of laterally inclined structures must be regarded as limited. However, these results are quite valuable in that they suggest a somewhat surprising structural pattern and should serve to guide future research into their nature.

The initial phases of part of this work were conducted under sponsorship of the National Science Foundation and the Office of Naval Research. Following phases were conducted under support of the Purdue Research Foundation. Their support is gratefully acknowledged.

REFERENCES

ALPER, A. & LIU, J. T. C. 1978 On the interactions between large-scale structure and fine grained turbulence in free shear flow. II. The development of spatial interactions in the mean. *Proc. R. Soc. Lond.* A **359**, 497–523.

ANTONIA, R. A., BROWNE, L. W. B., RAJAGOPALAN, S. & CHAMBERS, A. J. 1983 On the organized motion of a turbulent plane jet. *J. Fluid Mech.* **134**, 49–66.

BRADBURY, L. J. S. 1965 The structure of a self-preserving turbulent plane jet. *J. Fluid Mech.* **23**, 31–64.

BRADSHAW, P. 1966 The effects of initial conditions on the development of a free shear layer. *J. Fluid Mech.* **26**, 225–236.

BROWAND, F. K. 1966 An experimental investigation of the instability of an incompressible, separated shear layer. *J. Fluid Mech.* **26**, 281–307.

BROWAND, F. K. & WEIDMAN, P. D. 1976 Large scales in the developing mixing layer. *J. Fluid Mech.* **76**, 127–144.

BROWN, G. L. & ROSHKO, A. 1971 The effect of density difference on the turbulent mixing layer. *Turbulent Shear Flows, AGARD-CP*-93, 23(1–12).

BROWN, G. L. & ROSHKO, A. 1974 On density effects and large structure in turbulent mixing layers. *J. Fluid Mech.* **64**, 775–816.

CANTWELL, B. J. 1981 Organized motion in turbulent flow. *Ann. Rev. Fluid Mech.* **13**, 457–515.

CERVANTES DE GORTARI, J. G. 1978 An experimental study of the flapping motion of a turbulent plane jet. Ph.D. thesis, School of Mechanical Engineering, Purdue University.

CERVANTES DE GORTARI, J. G. & GOLDSCHMIDT, V. W. 1981 The apparent flapping motion of a turbulent plane jet – further experimental results. *Trans. ASME* I: *J. Fluids Engng* **103**, 119–126.

CHAMBERS, F. W. 1977 Acoustic interaction with a turbulent plane jet. Ph.D. thesis, School of Mechanical Engineering, Purdue University.

DAVIES, P. O. A. L. & YULE, A. J. 1975 Coherent structures in turbulence. *J. Fluid Mech.* **69**, 513–537.

EVERITT, K. W. & ROBINS, A. G. 1978 The development and structure of turbulent plane jets. *J. Fluid Mech.* **88**, 563–568.

FLORA, J. J. & GOLDSCHMIDT, V. W. 1969 Virtual origins of a free plane turbulent jet. *AIAA J.* **7**, 2344–2346.

FREYMUTH, P. 1966 On transition in a separated laminar boundary layer. *J. Fluid Mech.* **25**, 683–704.

GOLDSCHMIDT, V. W. & BRADSHAW, P. 1973 Flapping of a plane jet. *Phys. Fluids* **16**, 354–355.

GOLDSCHMIDT, V. W., YOUNG, M. F. & OTT, E. S. 1981 Turbulent convective velocities (broadband and wavenumber dependent) in a plane jet. *J. Fluid Mech.* **105**, 327–345.

GRANT, H. L. 1958 The large eddies of turbulent motion. *J. Fluid Mech.* **4**, 149–190.

GUTMARK, E. & WYGNANSKI, I. 1976 The planar turbulent jet. *J. Fluid Mech.* **73**, 465–495.

HESKESTAD, G. 1965 Hot-wire measurements in a plane turbulent jet. *Trans. ASME* E: *J. Appl. Mech.* **32**, 721–734.

HO, C. M. & HUANG, L. S. 1982 Subharmonics and vortex merging in mixing layers. *J. Fluid Mech.* **119**, 443–473.

HUSSAIN, A. K. M. F. & CLARK, A. R. 1977 Upstream influence on the near field of a plane turbulent jet. *Phys. Fluids* **20**, 1416–1425.

HUSSAIN, A. K. M. F. & HUSAIN, Z. D. 1979 Axisymmetric mixing layer: influence of the initial and boundary conditions. *AIAA J.* **17**, 48–55.

HUSSAIN, A. K. M. F. & REYNOLDS, W. C. 1970 The mechanics of an organized wave in turbulent shear flow. *J. Fluid Mech.* **41**, 241–258.

HUSSAIN, A. K. M. F. & ZEDA, M. F. 1978 Effects of the initial condition on the axisymmetric free shear layer: effects of the initial momentum thickness. *Phys. Fluids* **21**, 1100–1112.

KLEIS, S. J. & FOSS, J. F. 1974 The effect of exit conditions on the development of an

axisymmetric turbulent free jet. *3rd Year Tech. Rep., Grant NGR* 23-004-068. NASA Lewis Research Center.

KNISELY, C. & ROCKWELL, D. 1982 Self-sustained low frequency components in an impinging shear layer. *J. Fluid Mech.* **16**, 157–186.

LAU, J. C., FISHER, M. J. & FUCHS, H. V. 1972 The intrinsic structure of turbulent jets. *J. Sound Vib.* **22**, 379–406.

LAUFER, J. 1975 New trends in experimental turbulence research. *Ann. Rev. Fluid Mech.* **7**, 307–326.

LAUFER, J. 1981 *Transition and Turbulence*, pp. 63–76. Academic.

LAUFER, J. & MONKEWITZ, P. 1980 On turbulent jet flows: a new perspective. *AIAA Paper* 80-0962, Hartford, Conn.

MATTINGLY, G. E. & CRIMINALE, W. O. 1971 Disturbance characteristics in a plane jet. *Phys. Fluids* **14**, 2258–2264.

MICHALKE, A. 1965 On spatially growing disturbances in an inviscid shear layer. *J. Fluid Mech.* **23**, 521–544.

MIKSAD, R. W. 1972 Experiments on the nonlinear stages of free-shear-layer transition. *J. Fluid Mech.* **56**, 695–719.

MIKSAD, R. W. 1973 Experiments on nonlinear interactions in the transition of a free shear layer. *J. Fluid Mech.* **59**, 1–21.

MIKSAD, R. W., JONES, F. L. & POWERS, E. J. 1981 An approach to estimating spectral energy transfer due to nonlinear interactions. In *Proc. 7th Biennial Symp. on Turbulence, University of Missouri-Rolla*, pp. 401–408.

MIKSAD, R. W., JONES, F. L. & POWERS, E. J. 1983 Measurement of nonlinear interactions during natural transition of a symmetric wake. *Phys. Fluids* **26**, 1402–1409.

MIKSAD, R. W., JONES, F. L., POWERS, E. J., KIM, Y. C. & KHADRA, L. 1982 Experiments on the role of amplitude and phase modulations during transition to turbulence. *J. Fluid Mech.* **123**, 1–29.

MONKEWITZ, P. A. 1983 On the nature of the amplitude modulation of jet shear layer instability waves. *Phys. Fluids* **26**, 3180–3184.

MUMFORD, J. C. 1982 The structures of the large eddies in fully developed turbulent shear flows. Part 1. The plane jet. *J. Fluid Mech.* **118**, 241–268.

OLER, J. W. 1980 Coherent structures in the similarity region of a two-dimensional turbulent jet: a vortex street. Ph.D. thesis, School of Mechanical Engineering, Purdue University.

OLER, J. W. & GOLDSCHMIDT, V. W. 1982 A vortex-street model of the flow in the similarity region of a two-dimensional free turbulent jet. *J. Fluid Mech.* **123**, 523–535.

OSTER, D., WYGNANSKI, I., DZIOMBA, B. & FIEDLER, H. 1977 On the effect of initial conditions on the two-dimensional turbulent mixing layer. In *Structure and Mechanisms of Turbulence*, vol. I. Springer.

ROBINS, A. G. 1973 The development and structure of a two-dimensional free turbulent jet. Ph.D. thesis, Department of Aeronautics, Imperial College of Science and Technology.

ROCKWELL, D. O. & NICCOLLS, W. O. 1972 Natural breakdown of planar jets. *Trans. ASME* I: *J. Basic Engng* **94**, 72–730.

ROSHKO, A. 1976 Structure of turbulent shear flows: a new look. *AIAA J.* **14**, 1349–1357.

SATO, H. 1960 The stability and transition of a two-dimensional jet. *J. Fluid Mech.* **1**, 53–80.

SATO, H. 1970 An experimental study of non-linear interaction of velocity fluctuations in the transition region of a two-dimensional wake. *J. Fluid Mech.* **44**, 741–765.

SATO, H. & KURIKI, K. 1961 The mechanism of transition in the wake of a thin flat plate placed parallel to a uniform flow. *J. Fluid Mech.* **11**, 321–352.

SATO, H. & SAITO, H. 1975 Fine-sructure of energy spectra of velocity fluctuations in the transition region of a two-dimensional wake. *J. Fluid Mech.* **67**, 539–559.

SATO, H. & SAITO, H. 1978 Artificial control of the laminar–turbulent transition of a two-dimensional wake by external sound. *J. Fluid Mech.* **84**, 657–672.

SATO, H. & SAKAO, F. 1964 An experimental investigation of a two-dimensional jet at low Reynolds numbers. *J. Fluid Mech.* **20**, 337–352.

SCHLICHTING, H. 1934 *Z. angew. Math. Mech.* **14**, 368.

TENNEKES, H. & LUMLEY, J. L. 1972 *A First Course in Turbulence.* The M.I.T. Press.

THOMAS, F. O. 1983 Development of a two-dimensional turbulent jet under natural and excited conditions. Ph.D. thesis, School of Mechanical Engineering, Purdue University.

THOMAS, F. O. & GOLDSCHMIDT, V. W. 1983 Interaction of an acoustic disturbance and a two-dimensional turbulent jet: experimental data. *Trans. ASME* I: *J. Fluids Engng* **105**, 134–139.

THOMPSON, C. A. 1975 Organized motions in a plane turbulent jet under controlled excitation. Ph.D. thesis, University of Houston.

TOWNSEND, A. A. 1956 *The Structure of Turbulent Shear Flow.* Cambridge University Press.

WEIR, A. D. & BRADSHAW, P. 1975 Resonance and other oscillations in the initial region of a plane turbulent jet. *I.C. Aero Report* 75-07, Imperial College of Science and Technology, Department of Aeronautics.

WINANT, C. D. & BROWAND, F. K. 1974 Vortex pairing: the mechanism of turbulent mixing layer growth at moderate Reynolds number. *J. Fluid Mech.* **63**, 237–255.

YOUNG, M. F. 1973 A turbulence study: convective velocities, energy spectra and turbulent scales in a plane air jet. M.S. thesis, School of Mechanical Engineering, Purdue University.